

João Batista P. Falcão Filho*
Institute of Aeronautics and Space
São José dos Campos/SP – Brazil.
falcaojbpf@iae.cta.br

Maria Luísa Collucci C. Reis
Institute of Aeronautics and Space
São José dos Campos/SP – Brazil.
marialuisamlccr@iae.cta.br

Algacyr Morgenstern Jr.
Institute of Aeronautics and Space
São José dos Campos/SP – Brazil.
algacyramj@iae.cta.br

* author for correspondence

Experimental results from the sounding vehicle Sonda III test campaign in the Pilot Transonic Wind Tunnel

Abstract: *The Pilot Transonic Wind Tunnel of the Institute of Aeronautics and Space has conducted the first test campaign of a sounding vehicle, Sonda III. The campaign is part of a project whose activities and final results are presented in this paper. During the test campaign, many activities were performed to increase the productivity and accuracy of the tunnel. These activities included calibration procedures, corrective and preventive trials, development of auxiliary devices, and theoretical and experimental analysis. Two tasks are described in details: the development and tests performed with the static pressure probe and the automatic re-entry flap actuation system. Several tests were carried out with the Sonda III at Mach numbers ranging from 0.3 to 1.0, at stagnation pressures of 70, 94, and 110 kPa. Experimental results include global aerodynamic coefficients (using internal balance) and pressure distribution over essential regions of the test article (using pressure sensitive paint technique).*

Keywords: *Aerodynamics, Experimental results, Sonda III, Transonic Wind Tunnel.*

LIST OF SYMBOLS AND ACRONYMS

A :	Cross sectional area of fuselage
AEB:	Brazilian Space Agency
ALA:	Aerodynamics Division of IAE
AEDC:	Arnold Engineering Development Center
CD :	Drag coefficient
CD_0 :	Drag coefficient at zero angle of attack
CFD:	Computational fluid dynamics
CL :	Lift coefficient
C_m :	Pitching moment coefficient
Cl :	Roll moment coefficient
C_n :	Yawing moment coefficient
CNPq:	National Council for Scientific and Technological Development
CY :	Side force coefficient
DCTA:	Department of Aerospace Science and Technology
EEL:	Industrial Engineering College
FINEP:	Brazilian National Agency for the Financing of Project and Studies
IAE:	Institute of Aeronautics and Space
ITA:	Technological Institute of Aeronautics
ℓ :	Reference length
M :	Mach number
PIC:	Programmable microcontroller

PSP:	Pressure sensitive paint
q :	Dynamic pressure, defined by $0.5\rho_\infty V_\infty^2$
TTP:	Pilot Transonic Wind Tunnel
UNITAU:	University of Taubaté
UNIVAP:	University of Vale do Paraíba
USP:	University of São Paulo
VLS:	Satellite Launch Vehicle
V_∞ :	Velocity at free stream condition
ρ_∞ :	Static density at free stream condition
σ_M :	Standard deviation of Mach number

INTRODUCTION

The TTP of the IAE is a modern installation, built in 1997 and made operational in 2002. The tunnel has a conventional closed circuit and is continuously driven by an 830 kW main axial compressor and an intermittent injection system, which operates in a combined mode, for at least 30 seconds. Its test section is 300 mm wide and 250 mm high, with slotted walls, and it has automatic stagnation pressure controls (from 50 to 125 kPa), Mach number (from 0.2 to 1.3), stagnation temperature and humidity to properly simulate Mach and Reynolds numbers (Falcão Filho and Mello, 2002).

Figure 1 shows the operational envelope of the TTP, in which the test capacity of the tunnel in terms of Reynolds numbers related to a typical reference chord of 27.4 mm can be seen. The TTP is a 1/8th scale of an industrial transonic project. It was initially designed to study the innovative features of the industrial facility,

Received: 10/07/2011

Accepted: 04/10/2011

mainly concerning with the injection system operation in combination with the conventional main compressor operation. It was also designed to train the technical team to develop basic and academic research in high-speed regimes. Other activities include tests of vehicles with simple geometrical shapes, tests for the development of new aerodynamic transonic profiles, qualitative tests of airplanes with basic configurations, anemometric tests, amongst others. To accomplish this, the tunnel has three sets of six multi-component internal balances manufactured by MicroCraft™ for measuring forces and moments, four modules of 16 pressure channels scanners from PSI™ (2000) for pressure distribution tests, a Schlieren visualization system, hot-wire equipment, and PSP technique to determine pressure distribution over the model surface. In addition, the tunnel possesses a two-dimensional probe positioning system, angle of attack remotely controlled system and re-entry flap capability (Falcão Filho *et al.*, 2009).

Figure 2 shows a partial view of the aerodynamic circuit of the TTP along with some valves and tubing from the auxiliary systems, and the structural frame in grey, which



Figure 2. Partial view of the TTP aerodynamic circuit.

whose objective was to achieve know-how about sounding vehicles wind tunnel tests. Out of this amount, 48% were used in the product development, 47% in maintenance and 5% in consumables. The campaign lasted 46 months in contrast to the 41 originally planned, and it used the tunnel for an estimated 1,200 working hours.

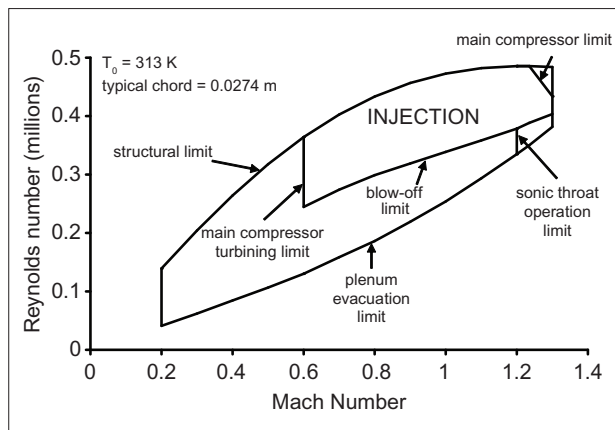


Figure 1. The operational envelope of the TTP.

is used to open the plenum chamber door. Technical details regarding the TTP can be found in Falcão Filho and Mello's (2002) paper.

As a transonic wind tunnel, the TTP is a suitable tool to investigate important effects in the transition range (Goethert, 1961). Particularly for the IAE sounding vehicles, some physical phenomena can be more precisely assessed and used for CFD code comparisons. This resulted in a proposal for a project, which was approved to run from 2007 to 2010. The AEB, by means of the VLS Associated Technology Projects, sponsored the activities of a complete test campaign with the sounding vehicle Sonda III, named “*Realização de Ensaios do VS-30 no Túnel Transônico Piloto do IAE*” (Tests Development with VS-30 in the IAE Pilot Wind Tunnel). An amount of BRL 271,981.57 was provided for the project,

Thus, the TTP technical team conducted a test campaign to assess the aerodynamic parameters of Sonda III, using an internal balance, and to investigate the pressure distribution using PSP (PSP technique) over important regions of the model, such as the ogive, the inter-stage area, and fins. The Sonda III vehicle is a sounding rocket developed by the IAE. This is a double stage vehicle with a 300 mm diameter second stage, capable of carrying a payload of approximately 100 kg up to an altitude of 600 km. It is one of the sounding rocket families named Sonda, which started with Sonda I, first launched in 1965. Sonda III was launched 27 times between 1976 and 2002. Two models were constructed to allow the installation of an internal balance inside the fuselage: a second stage model (scale 1:11) and a two-stage complete configuration model (scale 1:20). The internal balance was fixed to a sting structure to measure the model's aerodynamic global parameters: forces (lift, CL , drag, CD and side, CY) and moments (pitching, Cm , roll, Cl and yawing, Cn). General force and moment coefficients were calculated based on literature (Anderson, 2001), by Eq. 1 and 2:

$$C_{\text{Force}} = \frac{\text{Force}}{q A} \quad (1)$$

$$C_{\text{Moment}} = \frac{\text{Moment}}{q A \ell} \quad (2)$$

where:

A is a reference area, herein adopted as the maximum cross sectional area of the fuselage,

ℓ is a reference length, considered as the maximum fuselage diameter, and

q is a reference dynamic pressure, calculated from the free stream parameters (density and velocity), and given by Eq. 3:

$$q = \frac{1}{2} \rho_{\infty} V_{\infty}^2 \quad (3)$$

Figure 3 shows the scaled models utilized in the experiments, which have configurations of angle of fins equal to 0° , 2.5° and 5.0° .

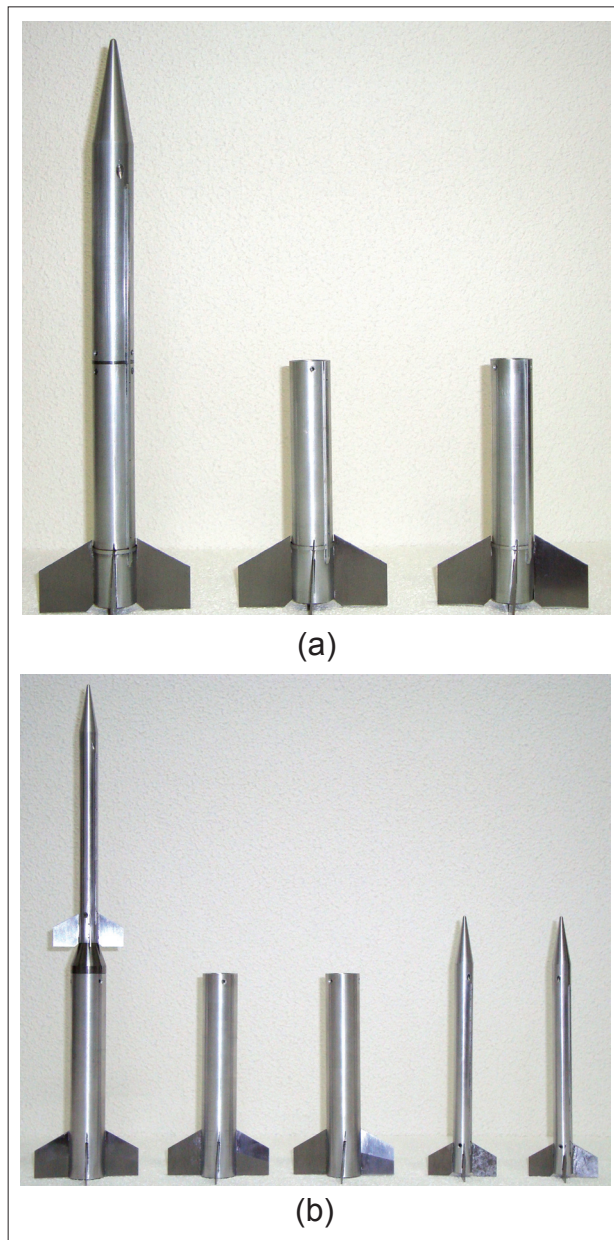


Figure 3. Sonda III: (a) second stage in scale 1:11 and (b) complete vehicle in scale 1:20 models.

During the test campaign, many activities were performed to increase the tunnel's productivity and accuracy of results. The present paper describes the main steps followed in implementing the project and some results obtained.

PRELIMINARY TASKS

Several procedures were undertaken during the campaign to better adapt the TTP for the proposed tests, which yielded important results that were then incorporated into the installation. Four different categories can be highlighted:

- (1) calibration procedures for the following: forced extraction mass flow from the plenum chamber, injection system operation with open and closed circuits, six-component internal balances with uncertainty determination, flow quality assessment in the test section, model's angle of attack setting of the model, and positioning of the re-entry flaps;
- (2) corrective and preventive maintenance procedures for several components and subsystems to guarantee the perfect operation of the tunnel throughout the campaign, such as the main frequency inverter, auxiliary compressors of injection system, circuit pressure and humidity controls, the cooling tower, the main motor gear lubrication, the auxiliary service air system, and cleaning of the aerodynamic circuit;
- (3) design development of pressure probe with 34 measuring channels to test section uniformity verification, calibration rig for multi-components internal balances loads application, two-dimensional platform for probe positioning, profile rotation device installed on the test section walls, blockage valve installed in the cooling water circuit, items for the pressure sensor scanner calibration, and plenum chamber opening mechanism;
- (4) carrying out of theoretical and experimental studies to improve the TTP test performances, such as determining the main parameters of the injection system and the polytropic coefficient of the reservoirs, designing a first-throat for Mach number 1.3, determining the operational parameters of the dryer system and the main parameters of the supersonic mixing chamber, as well as numerical simulations of NACA 0012 profile and Sonda III installed in the test section.

During the campaign, many scientific studies were presented at conferences, and the TTP team had the technical collaboration of undergraduate students from many universities (ITA, ETEP, UNIVAP, UNITAU, USP-São Carlos), under Scientific Initiation scholarships

sponsored by CNPq: Goffert *et al.* (2008a, 2008b), Zanin *et al.* (2008a, 2008b), Tagawa *et al.* (2008), Silva *et al.* (2009), Goffert and Falcão Filho (2008, 2009), Souza *et al.* (2009), Reis *et al.* (2009), Goffert *et al.* (2010), Silva *et al.* (2010), Souza *et al.* (2010), Vargas and Falcão Filho (2010), Costa *et al.* (2010), Schiavo *et al.* (2011), Silva *et al.* (2011), Falcão Filho and Ubertini (2011), Falcão Filho *et al.* (2011), Goffert *et al.* (2011).

Out of all the preliminary tasks conducted during the campaign, there are three very important ones worthy of mention: the internal balance calibration procedures, which are well documented in Tagawa *et al.* (2008) and Reis *et al.* (2008, 2009, 2010); the static pressure probe development; and the automatic re-entry flap actuation system. The last two will be further described.

According to Davis *et al.* (1986), the basic criterion to ensure good flow quality in modern transonic wind tunnels is given by the standard deviation of the Mach number over the nominal test section where the model is installed. The accuracy in this area must be periodically verified to guarantee the robustness and repeatability of the tests performed in the installation. The criterion for the standard deviation of the Mach number is described by Eq. 4:

$$|2\sigma_M| \leq 0.001 \quad (4)$$

A static pressure probe was developed to assess the Mach number distribution in the TTP. The probe is composed of an ogive tip with an outer diameter of 17.2 mm and a cylinder 1,240 mm in length. The blockage area ratio of the probe is 0.39%. On the surface of the probe, there are 33 static pressure tap stations. Each station is composed of four orifices, which are circumferentially distributed in a cross section area of the cylinder. The four orifices are interconnected, which provide a single static pressure value of the flow at each station location. One tap at the tip of the probe provides the total pressure. Pressure sensors located outside of the plenum chamber supply the pressure readings. Pressure taps holes of 0.5 mm diameter guarantee good accuracy of the pressure readings. The probe wall thickness is 2.1 mm to ensure sufficient rigidity to prevent the probe from bending. Figure 4 shows the probe installed in the test section. Thanks to the rigidity imposed on the design, total bending of only 0.5 mm at the tip was observed, which was practically unnoticeable in the nominal test section region.

Figure 5 shows the Mach number distribution along the central line of the test section measured by the static pressure probe. The test section re-entry flaps are closed and there is no forced mass extraction from the plenum chamber.

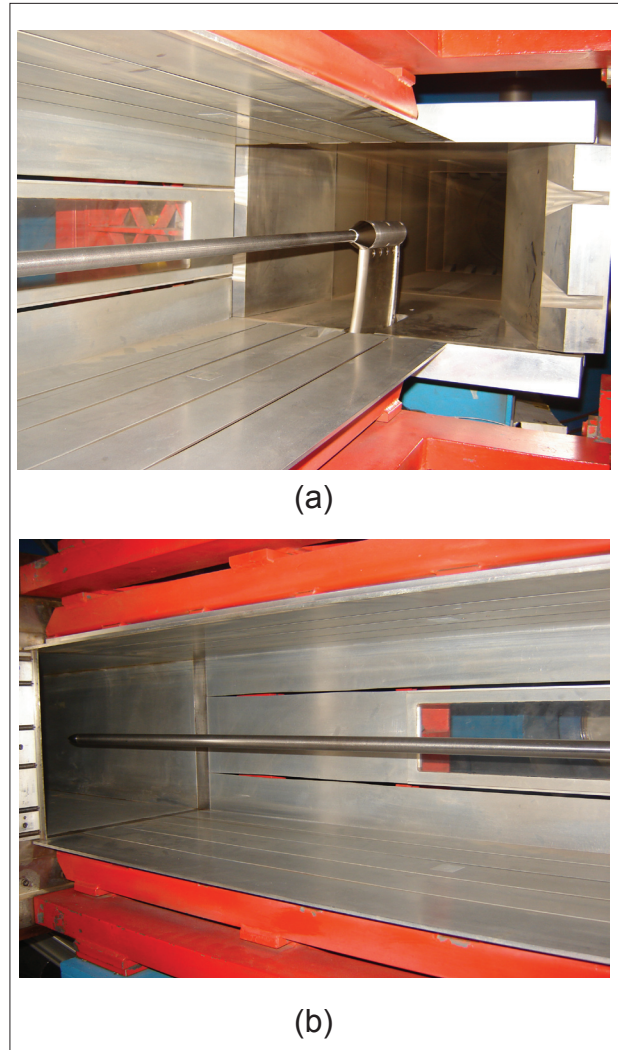


Figure 4. Static pressure probe installed in the test section showing: (a) the attachment to the angle of attack support, and (b) frontal part.

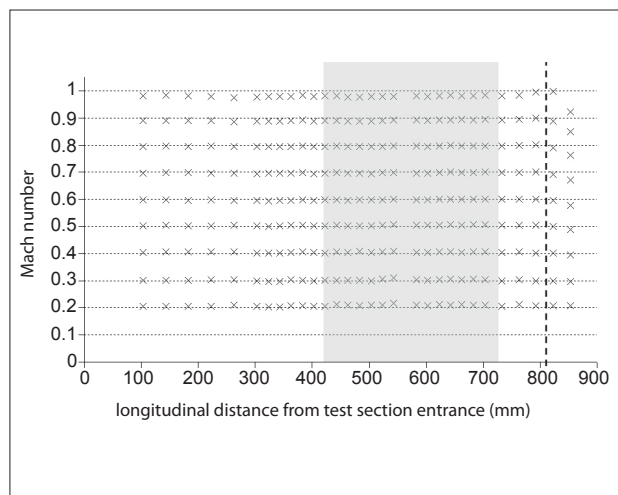


Figure 5. Distribution of the Mach number centerline (shaded area marks the nominal test section region).

The shaded area marks the nominal test section region and the dashed vertical line marks the test section end. Two measuring stations are located further along this line, in the flap region. Mach number values in this figure were obtained by taking an average value from the test runs data readings over a period of 60 seconds. Mach number deviation observed in the nominal test section region was about 0.002 for most of the operational conditions in the tunnel. It shows that there is good flow quality in the TTP, though still behind the modern state-of-art requirement established by Eq. 4. The test section wall convergent angle and the re-entry flap positioning angle can still be adjusted for better results, which will be carried out in a near future study.

A remote control system based on stepper motors for the two flap panels (located at each lateral wall just after the test section) was developed to improve the tunnel performance and productivity (Fig. 6a). In the past, the opening of the flap angles was manually adjusted by means of wheels that commanded a worm screw, as seen in Fig. 6b, and it was necessary to stop the test to manually operate the flaps command. As the tunnel circuit is pressurized, this procedure was very tedious and time consuming. Besides, in transonic tunnels, it is important to operate the re-entry flaps remotely to investigate optimum test conditions for each test configuration and model attitude. For example, at high angle of attack during polar movements, adjustment of the flaps may be necessary.

The flow chart in Fig. 7 shows the electronic components involved in the project to operate the stepper motors. The central microcomputer (1) located in the TTP control room, which is used to manage and monitor all subsystems actions in the tunnel, commands the flap to move to a determined angle. The signal is sent to the stepper motors (5) through auxiliary circuits (2), programmable microcontrollers named PIC (3) and power drivers (4). The PICs and the power drivers are supplied by a stable voltage source (6). Two hybrid stepper motors (5) were selected to operate in bi-polar and in series mode, since it is more appropriate for the driver utilized, with only two poles and with a lower raged current per phase. The power drivers chosen (4) with high performance receive signals from PICs (3). The signals are: clock, direction of movement and enabling, which command the stepper motors operation.

A PIC was chosen because it can be installed very close to the drivers and motors, thereby avoiding electrical noise. PICs are very popular due to their low cost, wide availability, large user base and programming, and re-programming capability. The microcontroller works as a remote logical unit, which receives data from the

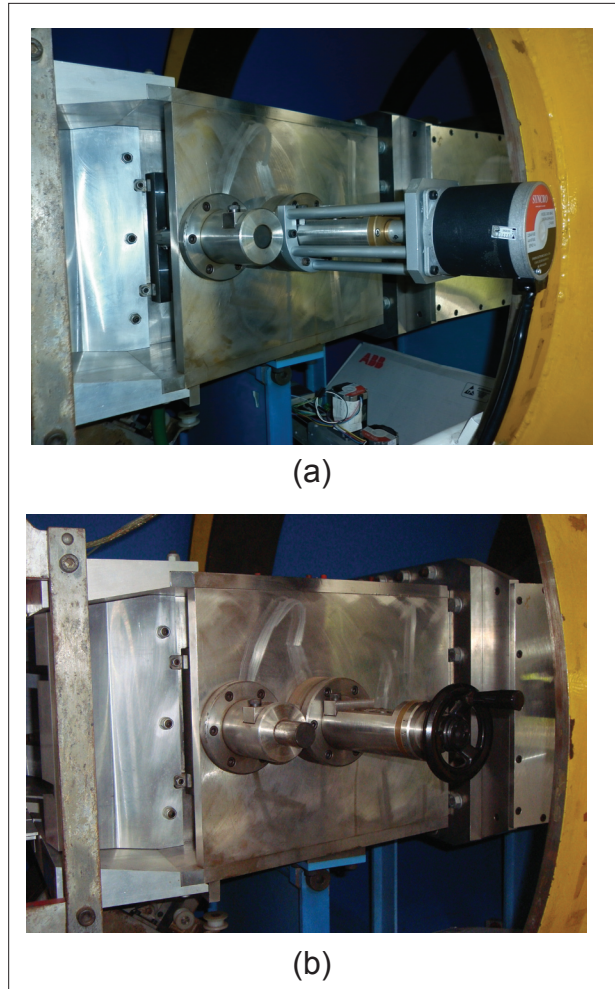


Figure 6. Re-entry flap actuation: (a) modified to remote control actuation, (b) original manual control.

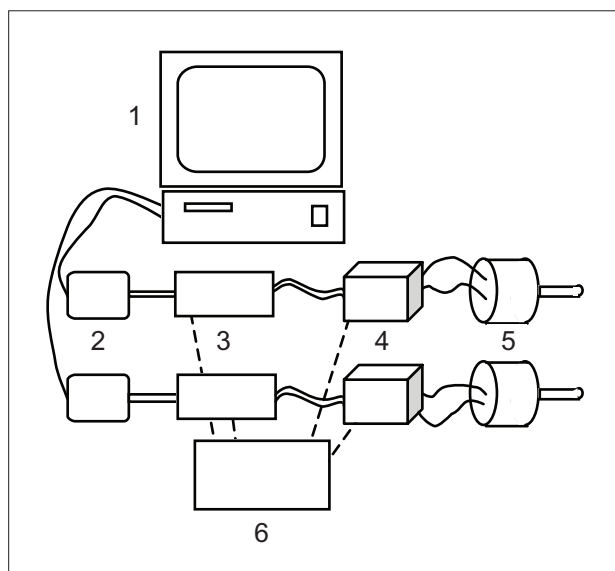


Figure 7. Electronic logical data transference for stepper motor control using PIC.

central microcomputer. Then, the central microcomputer is free to perform other tasks. The PIC was programmed by a code developed in Assembly language, recorded by a Microchip™ unit, in order to send instructions to the drivers. The code contains information to control the stepper motors: the amount of pulses to allow movement, which directions to take and to emit an emergency signal. Since this logic unit is close to the motors, the communication frequency may be higher without electronic noise, thus allowing a faster motor movement. A switched mode power source supplies the PICs and the power drivers. An auxiliary electronic circuit between the microcomputer and the PIC was introduced to control voltage level and optical isolation, for operational safety reasons.

The PIC receives instructions from the central microcomputer by means of a program developed in LabView®. This program reports the current positioning of the angle of flap. When the user wants to change this value, a warning signal in yellow displays the value of the flap positioning while the operation is in progress. The original white color is restored when the operation is completed. The conversion between the desired angle and the amount of pulses and motor rotation direction is embedded in this operation as well as a protocol for communication with the PIC. It was necessary to establish a relation between the angle position and the positioning ruler in the shaft. The opening flap angle can be monitored and changed during a tunnel test procedure. Its average speed is 0.7 degrees per second, which is adequate for all tests devised in the tunnel.

RESULTS FROM FORCE AND MOMENT

The second stage of the Sonda III model was tested for the entire range of Mach number (Reis *et al.*, 2010), even though only hypersonic regimes data are of real interest. However, the results for the complete vehicle at transonic range are very useful due to its flight at low altitude. Eighty aerodynamic polars were planned for the complete model varying the angle of attack from -5° to $+5^\circ$, for configuration of fins angle at 0° , 2.5° and 5.0° , related to the air direction. The Mach number range was from 0.2 to 1.0 for three stagnation pressure conditions: 70, 94 and 110 kPa.

For vehicles like Sonda III, which have jet exits at their rear, it is common to determine the aerodynamic coefficients data reduced to coefficients based on the assumption of zero base drag, *i.e.*, the axial force measured by the balance is subtracted from the model base area multiplied by the pressure difference between the measured value at the model base and at the free stream condition (Pope and Goin, 1978). Figure 8

shows the complete model of Sonda III in scale 1:20 installed in the test section of TTP, with one end of the internal balance connected to the model and the other one to the sting, which is fixed to a semi-circular sector of angle of attack positioning. The diagram in the figure clarifies the balance installation. Two pressure taps were installed at the rear part of the model to measure the base pressure, by taking an average of both taps. For all data herein reported, the assumption of zero base drag was applied.

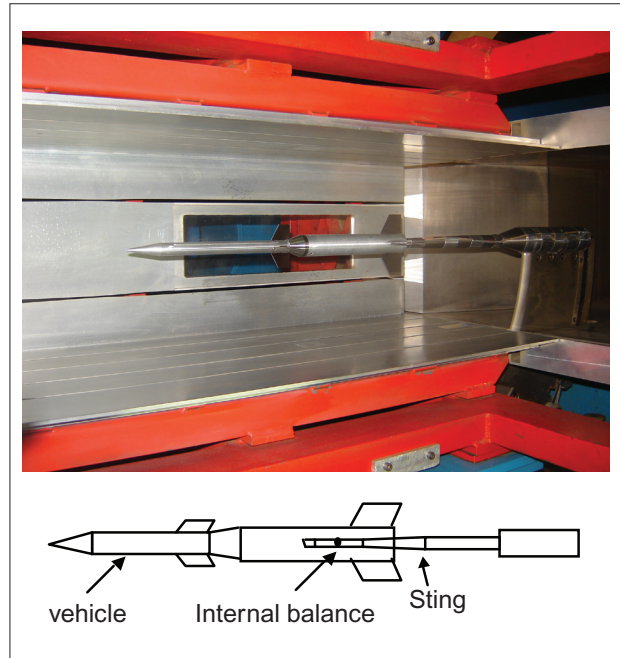


Figure 8. Sonda III complete model in scale 1:20 installed in the test section of the TTP and balance installation scheme.

The forces read by the internal balance had to be reduced to tunnel wind direction to obtain the lift and drag coefficients. Considering that the model is well aligned and the yaw angle is negligible, one can write (Pope and Goin, 1978):

$$F_L = F_N \cos \alpha - F_A \sin \alpha \quad (5)$$

$$F_D = F_N \sin \alpha + F_A \cos \alpha \quad (6)$$

where:

F_N and F_A are the forces read by the internal balance, in its normal and axial direction, respectively,

F_L and F_D the forces in the normal and axial directions relative to the wind direction, *i.e.*, lift and drag, as they are defined, and

α is the model angle of attack.

It is important to observe that the internal balance has small deflections under stress and, during the tests, this effect on the angle of attack measurement was not considered.

Finally, in order to obtain the correct value of aerodynamic forces and moments, many influences should be considered, such as: model support influence, upwash, downwash, buoyancy effects, and model blockage area ratio influence. In a transonic wind tunnel, many of these effects may be diminished by adjusting the flow conditions in the test section, actuating in the wall deflection and in the opening angle of re-entry flaps. In most cases, it is possible to obtain good results in transonic wind tunnels simply by ensuring that the blockage area ratio is kept below 1% (Pope and Goin, 1978). The data presented herein represent the first approach for the aerodynamic loads determination for Sonda III, as no other correction was employed. However, since the blockage area ratio of the model is 0.81% and the tunnel was adjusted to typical operational conditions of flaps opening (10°), reliable results are expected for low Mach numbers ($M_\infty < 0.7$) and reasonable results for higher speeds.

All the tests were performed using an internal balance with the following load limits of force: 160 N normal, 16 N axial and side; and moments: 24 Nm pitch, 16 Nm roll and yaw. The balance was calibrated in a rig with dead loads applied to obtain the calibration matrix to be used for data reduction (Reis *et al.*, 2009). The Mach number range was from 0.3 to 1.0, the stagnation pressure was 70, 94 and 110 kPa, and the model was installed in the test section in two different configurations: one with the fins oriented in “+” and the other in “x”, turned 45° in relation to the former.

Figure 9 shows the CD variation at zero angle of attack with the model in “+” configuration. Results were as expected, characterized by a constant value for low Mach numbers and growing as it approaches sonic Mach number (for $M \geq 0.8$). No appreciable differences can be observed with the variation of stagnation pressure, *i.e.*, with the variation of Reynolds number.

Figure 10 shows drag curves as a function of angle of attack for Mach number 0.80 for the model with fins at zero degree and in “+” configuration, with stagnation pressures of 70, 94 and 110 kPa. The general appearance of the curves is quite close to the theoretical prediction, with a curve that has a parabolic tendency. It is observed that the Reynolds number variation (stagnation pressure) has not caused a significant impact on the curves. It can also be seen that the curve for 70 kPa presented some oscillation, because during the tests this low pressure value could not be kept very stable.

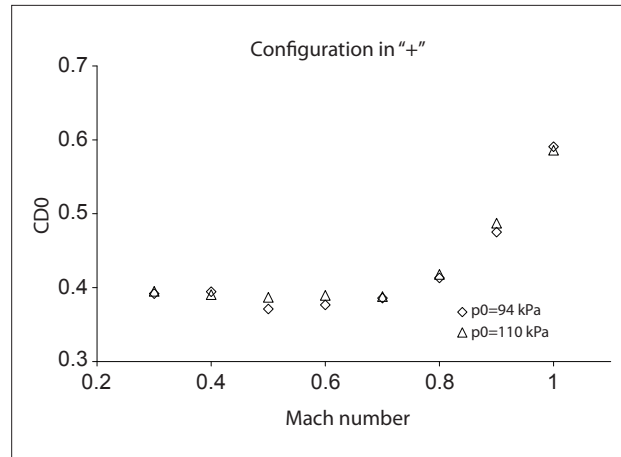


Figure 9. CD at zero angle of attack for “+” configuration with fins at zero degree for stagnation pressures at 94 and 110 kPa.

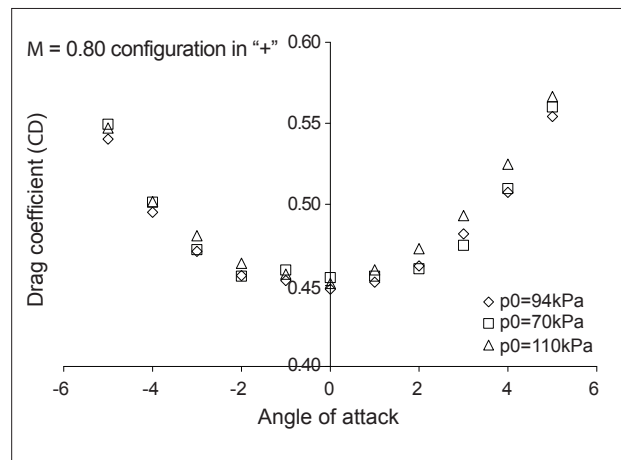


Figure 10. CD for Mach number 0.80, for configuration in “+”, and with fins at zero degree for stagnation pressures of 70, 94, and 110 kPa.

Figure 11 shows a typical result of the variation of the CL with respect to the angle of attack for Mach number 0.5, with stagnation pressure of 94 kPa, fins at 0 degree of deflection and configuration in “+”. The sequence followed in positioning the angle of attack was 0°, 1°, 2°, 3°, 4°, 5°, 4°, 3°, 2°, 1°, 0°, -1°, -2°, -3°, -4°, -5°, -4°, -3°, -2°, -1° and 0°. It is interesting to repeat some angle positions in order to check the repeatability of the tests. The curve shows a likeness to the theoretical prediction (polynomial of third degree) with a hysteresis effect almost nonexistent. In general, the curves for other test conditions showed similar trend.

Figure 12 shows a comparison of typical curves of CL , for configuration in “+”, fins at 0 degree and stagnation pressure of 94 kPa. Here again the third-degree polynomial behavior of the curves is very clear. It is also observed that the curves do not pass

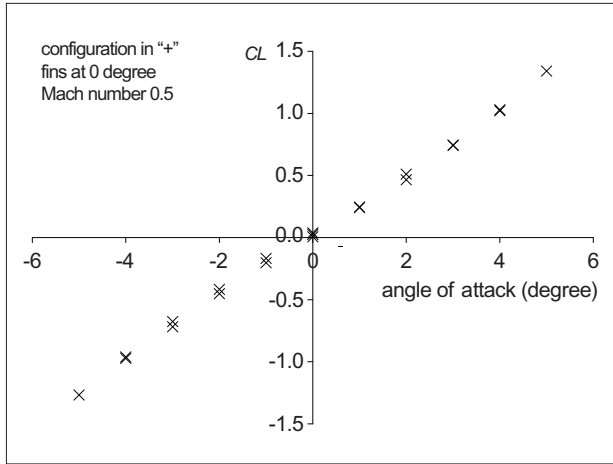


Figure 11. *CL* for configuration in “+”, fins at 0 degree of deflection, Mach number 0.5, and stagnation pressure of 94 kPa.

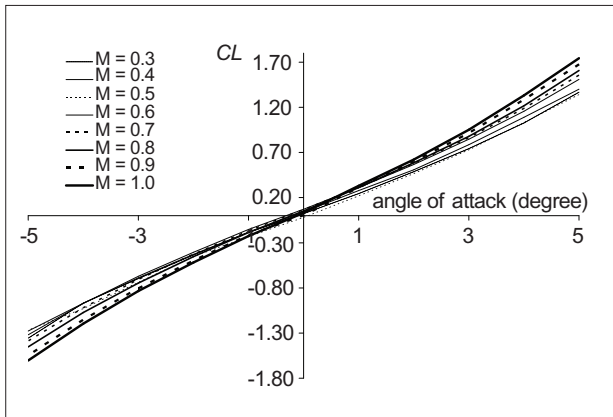


Figure 12. *CL* for configuration in “+”, fins at 0 degree, and stagnation pressure of 94 kPa.

perfectly through the origin, indicating a possible small misalignment of the model relative to the airflow, since the model is axisymmetric.

It is common to represent lift and drag in the same graphic, with a variation of the angle of attack. This graphic is called drag polar and, in Fig. 13, polar curves for all Mach numbers, for configuration in “x”, fins angle at 0 degree and stagnation pressure of 94 kPa are represented. All curves related to low Mach number are practically coincident. For Mach number equals and greater than 0.8, there is a noticeable increase of *CD*.

Figure 14 shows the *CY*, for the “+” configuration, fins at zero degree of deflection, stagnation pressure of 94 kPa, and for angle of attack sweep of: 0°, 1°, 2°, 3°, 4°, 5°, 4°, 3°, 2°, 1°, 0°, -1°, -2°, -3°, -4°, -5°, -4°, -3°, -2°, -1° and 0°. A zero value throughout the range was expected, however a *CY* of about 0.02 at -5° of angle of attack up to 0.06 at +5° of attack can be observed. This indicates that the angle of attack mechanism travels in

an irregular plane. But, considering the value of 0.06, it is possible to associate the same effect to the normal direction. In this way, a corresponding angle of attack of 0.1 degree causes an increase of about 0.06 in *CL*. A misalignment of 0.1 degrees represents a total of 0.7 mm linear misalignment between the extremities of the model, which could not be observed by the available alignment device. In Fig. 14 the hysteresis effect is practically undetectable. The same behavior was observed for all other flow conditions.

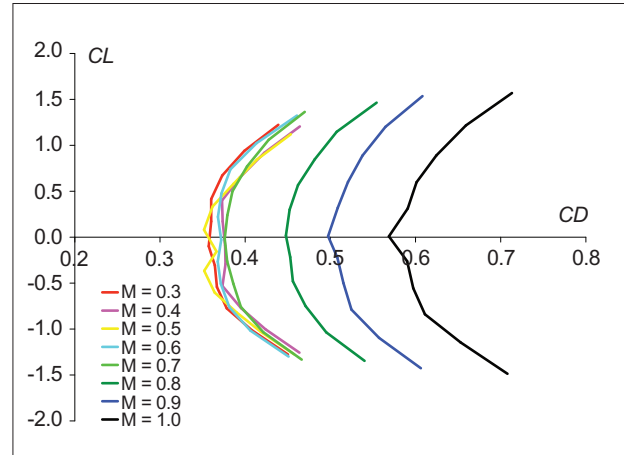


Figure 13. Polar ‘lift-drag’ for configuration in “x”, fins at 0 degree and stagnation pressure of 94 kPa.

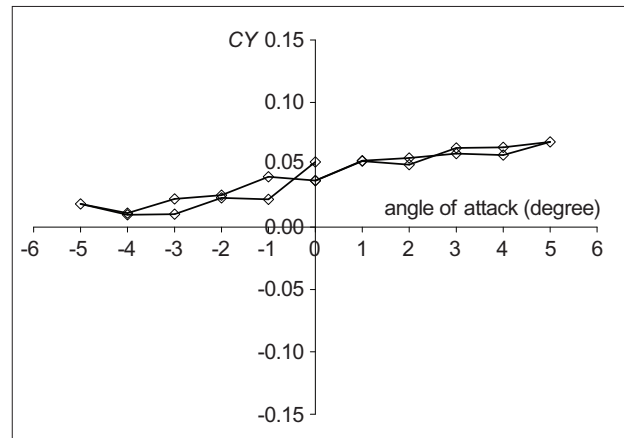


Figure 14. *CY* in the “+” configuration, fins at zero degree of deflection, and stagnation pressure of 94 kPa.

Figure 15 shows the average *CY*s and their standard deviation for all 80 test runs. From run 1 to 24, the model was in configuration in “+” and from 25 to 48 in “x”. No significant variation of *CY* was observed, indicating that the model’s axisymmetric feature was observed. However, as already observed, the value reflects a misalignment of about 0.7 mm along the model’s body. From runs 49 to 80, the model underwent

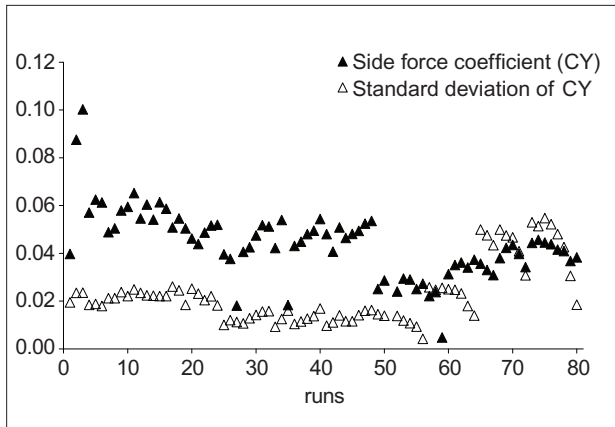


Figure 15. Average C_Y and corresponding standard deviation for all 80 runs.

several modifications from “x” to “+” and it also had parts with different fin angles changed (Fig. 3b). For these runs, one can observe a little decrease in the average C_Y but an increase in the standard deviation. It is possible to conclude that the tunnel support had, in fact, a misalignment of about 0.1 degree, which means that repair actions must be carried out to achieve better results.

A similar investigation was performed for the C_l , as shown in Fig. 16. From runs 1 to 48 the model’s fins were at 0 degrees of deflection, from 49 to 64 at 2.5 degrees of deflection and from 65 to 80 at 5.0 degrees of deflection, as can be clearly seen in the figure. The observed standard deviations were very small for all runs. However, for fins at 0 degrees the average value for some runs was very different from the expected zero value, related to low Mach number (0.3, 0.4 and 0.5), indicating that a more precise internal balance should be used for these low flow conditions.

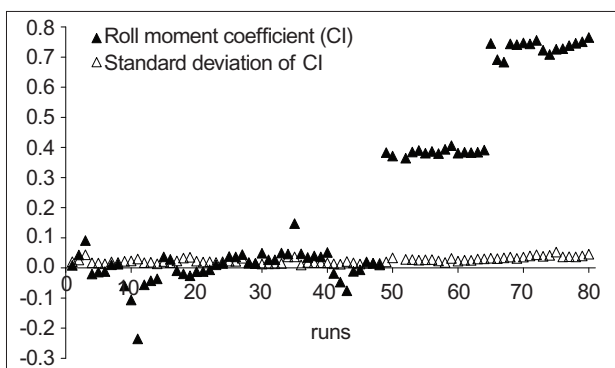


Figure 16. Average C_l and its standard deviation, for all 80 runs.

Figure 17 shows a comparison of C_m for the “+” and “x” configurations for Mach number 0.8 and stagnation pressure of 94 kPa. It is interesting to note that with the

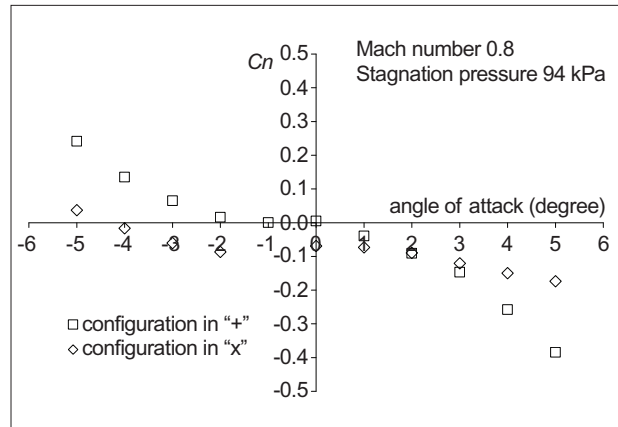


Figure 17. C_l for the “+” and “x” configurations.

“+” configuration, the curve presented a typical stable third-degree polynomial curve behavior with angle of attack variation, and crossing the origin of the graph. For the “x” configuration the same third-degree polynomial curve behavior was present (rotated counterclockwise from “+” configuration) and the curve does not pass through the origin. The influence of the fins in the “x” configuration is clear.

It is possible to determine an equation to be added to the values from configuration “+” to obtain the values from configuration “x”, given by Eq. 7.

$$C_n = -0.05 + 0.03\alpha \quad (7)$$

where:

α is the angle of attack.

RESULTS FROM PRESSURE DISTRIBUTION

Tests at some Mach number conditions were performed to determine pressure distribution over the second stage model, using the PSP technique.

Figure 18 shows an image obtained with PSP technique, for the front region of the model at angle of attack 0 degree and Mach number 1.0. The free stream static pressure is 49.6 kPa and in Figure 18 a graphic of the pressure distribution along the line traced in the PSP image can be seen. In the graphic, it is possible to observe an abrupt pressure decrease just after the cone end. From the local lowest pressure value of 28.0 kPa it is possible to approximately determine the maximum Mach number, which is equal to 1.44 at the expansion. The pressure rises up to the final level of 48.6 kPa at the recovery region, which corresponds

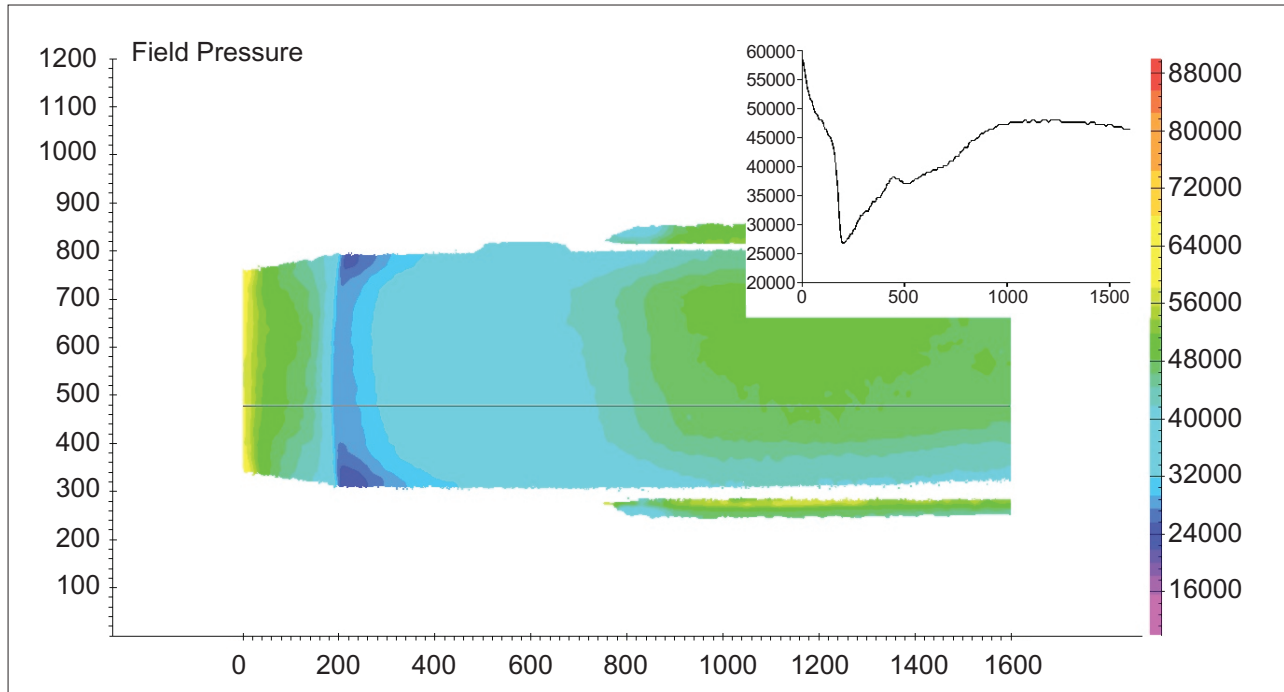


Figure 18. Image obtained with PSP technique showing pressure distribution over the model front region surface, at Mach number 1.0 and angle of attack of 0 degree.

to Mach number 1.0. One conventional pressure tap was drilled at the model fuselage, at 148 mm from the nose tip of the fuselage, which was connected to a pressure sensor. The pressure measured by the sensor was 0.230 kPa higher than the value obtained by the PSP technique, representing a very low relative error of 0.5%.

Figure 19 shows the same region for all Mach numbers in the range from 0.3 to 1.0. It is interesting to observe that the expansion region grows when the Mach number increases. For free stream Mach number of 0.8, 0.9 and 1.0, the maximum local Mach number values found were 1.17, 1.45 and 1.55, respectively.

Figure 20 shows an image of inter-stages regions of the complete model at Mach number 0.7 and angle of attack of zero degree. Two plateaus of pressure values were observed on the fuselage. One at the second stage (pressure about 73.0 kPa), and the other at the first stage (pressure about 71.0 kPa). The plateau in the second stage has a value that is a little higher and grows with the proximity of the inter-stage cone. This can be explained by the cone influence at subsonic Mach number and by the presence of fins. The pressure at the inter-stage cone was greater, as expected, approximately 19%, and the Mach number decreased to 0.46. In the expansion region, the sudden pressure decrease indicates a local Mach number of

about 0.93 (indicated by the narrow dark blue color vertical strip in Fig. 20).

CONCLUSIONS

The main activities related to the first test campaign of the sounding vehicle Sonda III from IAE held in TTP were described. The main tunnel characteristics and model configurations were described, as well as the internal balance used. The preliminary tasks undertaken to the tunnel installation were presented, and important developments were described in more details. They are as follows:

- The pressure probe to assess the flow quality in the test section, showing the longitudinal Mach number distribution for the whole Mach number range; and
- The implementation of automatic control for the re-entry flaps that optimizes the tunnel testing procedures, along with a description of the main features of the design in which a programmable microcircuit is used.

Important results of global aerodynamic loads and pressure distribution over the model surface were presented. Since completely accurate procedures of testing corrections for the tunnel were not yet developed, optimum expected conditions were applied to the tunnel controls and good

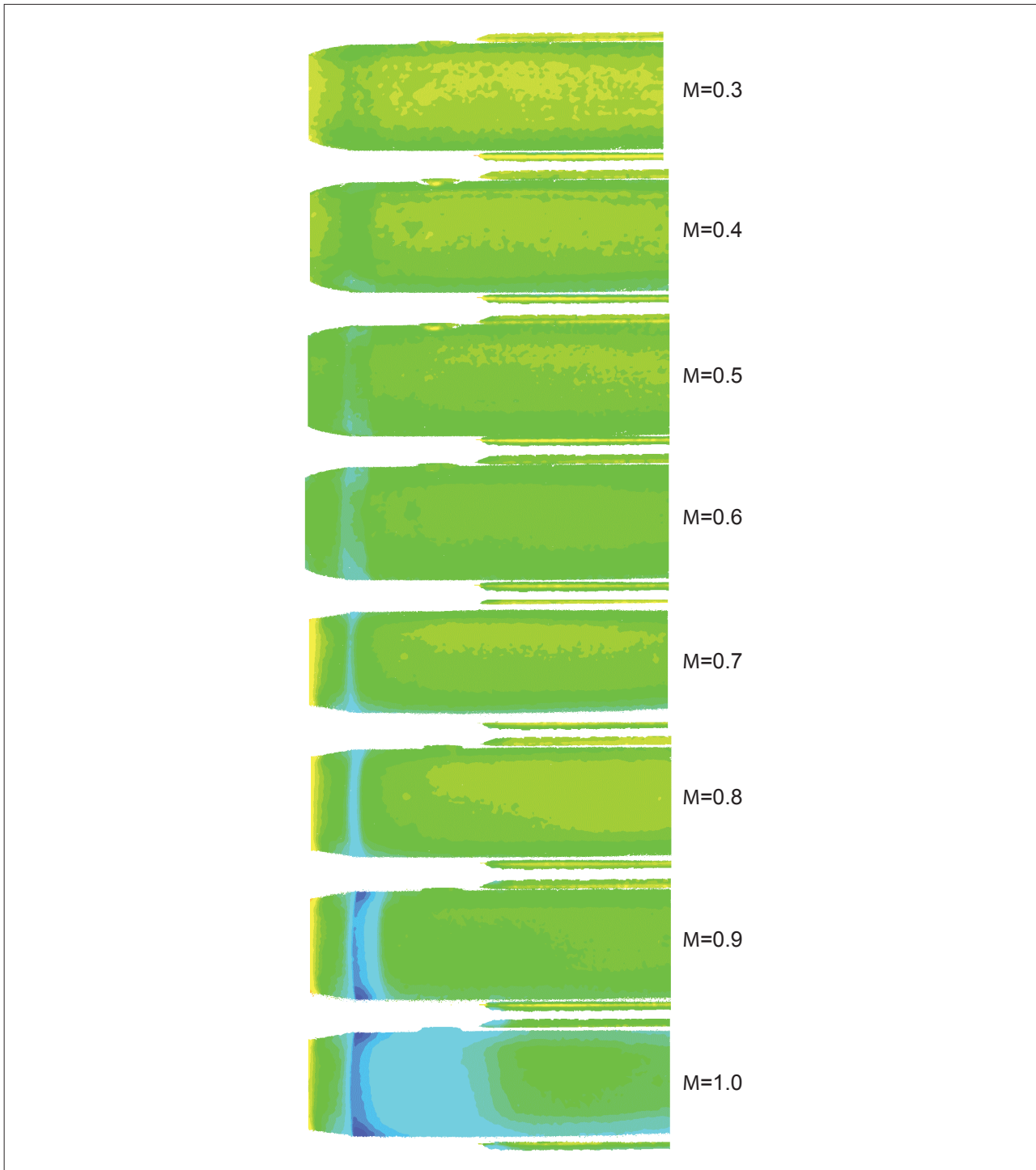


Figure 19. Images obtained with PSP technique showing pressure distribution over the model front region surface, at Mach number from 0.3 to 1.0 and angle of attack at 0 degree.

results are envisaged using a model in scale 1/20, with a 0.8% of blockage area ratio.

Global load coefficients were determined for Mach number range from 0.3 to 1.0 and stagnation pressure of 70, 94 and 110 kPa, for a complete version of the model, with

configurations of fins at 0° , 2.5° and 5.0° of deflection, and varying the angle of attack from -5° to $+5^\circ$. The curve of CD_0 indicated a CD of about 0.39 from Mach number of 0.3 to 0.7, reaching 0.59 at Mach number 1. The presented curves of CD_0 , $CD \times \alpha$, CL , and Cm were in accordance with the theoretical predictions. Curves of CY were used

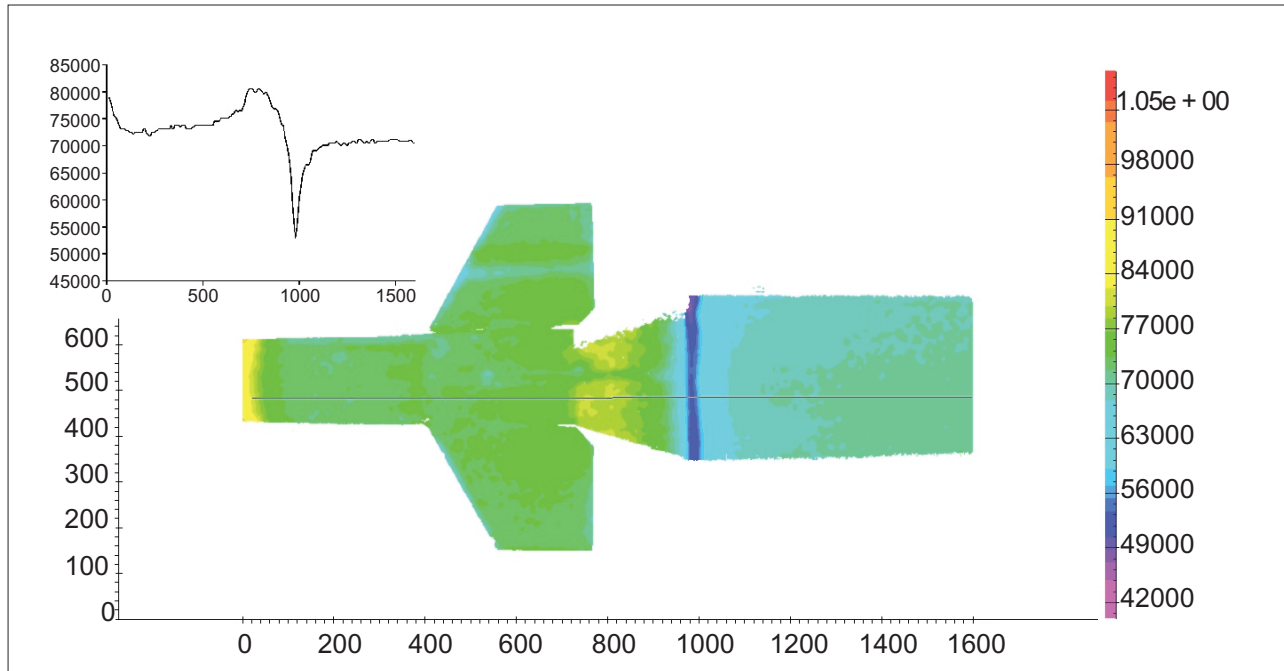


Figure 20. Image obtained with PSP technique showing pressure distribution over inter-stage region of the model at Mach number 0.7 and stagnation pressure of 94 kPa, and angle of attack zero degree.

to verify the alignment conditions in the test section. A misalignment of about 0.1 degree was found, which did not compromise the accuracy for the whole campaign, but this fact will be investigated in more details in the future. No appreciable impact was observed with stagnation pressure (Reynolds number) variation. A noticeable change could be seen in the curve of C_m when the model was changed from the “+” to the “x” configurations, due to the aerodynamic influence of the fins.

PSP was used to determine the pressure distribution over essential regions of the model, such as the ogive, inter-stage sector, and fins. The Mach number for expansion regions that is an important feature in wind tunnel testing was determined.

A very important step was taken with the conclusion of the present test campaign, enabling the technical team of TTP to proceed with aerodynamic testing in transonic range for models of real interest for the Brazilian aerospace industry.

ACKNOWLEDGMENTS

The authors are thankful to the AEB for the financial support of project 44 0000 “*Realização de Ensaios do VS-30 no Túnel Transônico Piloto do IAE*”, and to CNPq under grants 103520/2007-4, 101945/2007-8, 103518/2007-0, 101945/2007-8, 100656/2009-9, 103551/2008-5, 113853/2007-6, 104775/2008-4, 119235/2009-9, 119242/2009-5, 102506/2010-8, 106254/2008-1.

REFERENCES

- Anderson, J.D. Jr., 2001, “Fundamentals of Aerodynamics”, McGraw-Hill Higher Education, 3rd Edition, New York.
- Costa, R. S., Avelar, A. C., Falcão Filho, J. B. P., 2010, “Pressure Measurements Over a NACA 0012 Profile in a Transonic Wind Tunnel Using Pressure Sensitive Paint (PSP)”, Proceedings from 13rd Brazilian Congress of Thermal Sciences and Engineering, Uberlândia, Minas Gerais, Brasil.
- Davis, M. W., Gunn, J. A., Herron, R. D., Kraft, E. M., 1986, “Optimum transonic wind tunnel,” AIAA 14th Aerodynamic Testing Conference, 14, West Palm Beach, AIAA-86-0756-CP.
- Falcão Filho, J. B. P., Mello, O. A. F., 2002, “Descrição Técnica do Túnel Transônico Piloto do Centro Técnico Aeroespacial,” Anais ... IX Congresso Brasileiro de Ciências Térmicas e Engenharia, ENCIT-2002, Caxambu-MG, artigo CIT02-0251.
- Falcão Filho, J. B. P., Avelar, A. C., Reis, M. L. C. C., 2009, “Historical Review and Future Perspectives for the PTT – IAE Pilot Transonic Wind Tunnel,” Journal of Aerospace and Technology and Management, ISSN 1984-9648, Vol. 1, No. 1.
- Falcão Filho, J. B. P., Ubertini, G. P. A., 2011, “Pressure Probe Development and Tests in a Transonic Wind

Tunnel Calibration,” proceedings from 21st Brazilian Congress of Mechanical Engineering, Natal, RN, Brazil (accepted for publication).

Falcão Filho, J. B. P., Souza, F. M., Oliveira Neto, P. J., Rocha, A., Lima, D. S. A., 2011, “Automatic Control of Flaps in a Transonic Wind Tunnel Installation,” proceedings from 21st Brazilian Congress of Mechanical Engineering, Natal, RN, Brazil (accept for publication).

Goethert, B. H., 1961, “Transonic Wind Tunnel Testing”, Pergamon Press, New York.

Goffert, B., Tagawa, G. B. S., Zanin, R. B., Reis, M. L. C. C., Falcão Filho, J. B. P., 2008a, “Ensaio de Calibração de Turbina de Inserção do Sistema de Extração Forçada de Massa do Túnel Transônico Piloto do IAE”, Anais ... V Congresso Nacional de Engenharia Mecânica, CONEM-2008, Salvador-Bahia, artigo 0941.

Goffert, B., Truys, C. F., Lima, D. S. A., Falcão Filho, J. B. P., 2008b, “Control of Injection System for the Pilot Transonic Wind Tunnel of IAE in Closed Circuit”, Proceedings ... XII Brazilian Congress of Thermal Engineering and Sciences, ENCIT-2008, Belo Horizonte-MG, article 1-5054.

Goffert, B., Falcão Filho, J. B. P., 2008, “Determinação do Coeficiente Politrópico Associado aos Reservatórios de Ar Comprimido do Túnel Transônico Piloto do IAE”, Anais ... V Congresso Nacional de Engenharia Mecânica, CONEM-2008, Salvador-Bahia, artigo 1029.

Goffert, B., Falcão Filho, J. B. P., 2009, “Euler Equations Applied to Flow Over NACA 0012”. In: International Congress of Mechanical Engineering, 2009, Porto Alegre - RS. Anais do COBEM 2009 - COB09-1136, 2009.

Goffert, B., Vargas, M. M., Falcão Filho, J. B. P., 2010, “Verification and Validation of Laminar Navier-Stokes Applications,” Proceedings from 13rd Brazilian Congress of Thermal Sciences and Engineering, Dec. 05-10, Uberlândia, Minas Gerais, Brasil.

Goffert, B., Ubertini, G. P. A., Falcão Filho, J. B. P., 2011, “Design of a Supersonic First-Throat for a Transonic Wind Tunnel and Numerical Evaluation,” proceedings from 21st Brazilian Congress of Mechanical Engineering, Natal, RN, Brazil (accepted for publication).

Pope, A., Goin, K. L., 1978, “High-Speed Wind Tunnel Testing”, John Wiley & Sons, New York.

PSI, 2000, “ESP-16BP Pressure Scanner User’s Manual,” Catálogo de produto da firma Esterline Pressure Systems, 3rd Edition, Retrieved in June 10th, 2011, from www.pressuresystems.com.

Reis, M. L., Castro, R. M., Falcão Filho, J. B. P., Mello, O. A. F., 2008, “Calibration Uncertainty Estimation for Internal Aerodynamic Balance”, Proceedings ... 12th IMEKO TC1-TC7 joint Symposium on Man, Science & Measurement, Annecy, France.

Reis, M. L. C. C., Falcão Filho, J. B. P., Paulino, G., Truys, C., 2009 “Aerodynamic Loads Measurement of a Sounding Rocket Vehicle Tested in Wind Tunnel,” XIX IMEKO World Congress, Fundamental and Applied Metrology, September 6/11, 2009, Lisbon, Portugal.

Reis, M. L. C. C., Falcão Filho, J. B. P., Mello, O. A., 2010, “Wind Tunnel Tests of the Sonda III Aerospace Vehicle,” Anais do VI Congresso Nacional Engenharia Mecânica, 18 a 21 de agosto, Campina Grande, Paraíba, Brasil.

Schiavo, L. A. C. A., Reis, M. L. C. C., Falcão Filho, J. B. P., Truys, C. F., 2011, “Aerodynamic Tests of the AGARD Model B in a Transonic Wind Tunnel,” proceedings from 21st Brazilian Congress of Mechanical Engineering, Natal, RN, Brazil (submitted).

Silva, A. F. C., Braz, R. O., Avelar, A. C. B. J., Falcão Filho, J. B. P., 2009, “Study of the Mach Number Uniformity Over a Horizontal Plane Inside the Test Section of a Wind Tunnel,” In: International Congress of Mechanical Engineering, 2009, Porto Alegre - RS. Anais do COBEM 2009 - COB09-1053.

Silva, A. F. C., Ortega, M. A., Falcão Filho, J. B. P., 2010, “Diffuser Design for a Supersonic/Subsonic Mixing Chamber,” Proceedings from 13rd Brazilian Congress of Thermal Sciences and Engineering, Dec. 05-10, Uberlândia, Minas Gerais, Brasil.

Silva, A. F. C., Godinho, M. B. C., Ortega, M. A., Falcão Filho, J. B. P., 2011, “Supersonic/Subsonic Mixing Chamber Experimental Analysis,” proceedings from 21st Brazilian Congress of Mechanical Engineering, Natal, RN, Brazil (accepted for publication).

Souza, F. M., Falcão Filho, J. B. P., De Oliveira Neto, P. J., 2009, “First Throat Design of a Transonic Wind Tunnel,” In: International Congress of Mechanical Engineering, 2009, Porto Alegre - RS. Anais do COBEM 2009 - COB09-1142.

Souza, F. M., Neto, P. J. O., Silva, A. R., Lima, D. S. A., Reis, M. L. C. C., Falcão Filho, J. B. P., 2010,

“Metodologia de Calibração de Sistema de Medida de Pressão em Túneis de Vento,” Anais do VI Congresso Nacional de Engenharia Mecânica, 18 a 21 de agosto, Campina Grande, Paraíba, Brasil.

Tagawa, G. B. S., Reis, M. L. C. C., Falcão Filho, J. B. P., 2008, “Ajuste de Curva de Calibração de uma Balança Interna Multi-Componente”, Anais ... V Congresso Nacional de Engenharia Mecânica, CONEM-2008, Salvador-Bahia, artigo 1124.

Vargas, M. M., Falcão Filho, J. B. P., 2010, “Análise Numérica Bidimensional do Escoamento em Modelo de Veículo de Sondagem,” Anais do VI Congresso Nacional

de Engenharia Mecânica, 18 a 21 de agosto, Campina Grande, Paraíba, Brasil.

Zanin, R. B., Reis, M. L. C. C., Falcão Filho, J. B. P., 2008a, “Análise da Uniformidade Longitudinal do Número de Mach na Seção de Testes do Túnel Transônico Piloto do IAE em Circuito Aberto”, Anais ... V Congresso Nacional de Engenharia Mecânica, CONEM-2008, Salvador-Bahia, artigo 1031.

Zanin, R. B., Braz, R., Avelar, A. C. B. J., Falcão Filho, J. B. P., 2008b, “Analysis of the Drier System of the Pilot Transonic Wind Tunnel of IAE”, Proceedings ... XII Brazilian Congress of Thermal Engineering and Sciences, ENCIT-2008, Belo Horizonte-MG, article 1-5117.